Simultaneous oxidation and decarburization of cast iron powder during plasma spraying

K. Voleník[1]*, O. Schneeweiss[2], T. Chráska[1], J. Dubský[1], J. Písačka[1]

[1] *Institute of Plasma Physics AS CR, v.v.i., Za Slovankou 3, 182 00 Prague 8, Czech Republic*
[2] *Institute of Physics of Materials AS CR, v.v.i., Žižkova 22, 616 62 Brno, Czech Republic*

Received 3 July 2008, received in revised form 12 September 2008, accepted 12 September 2008

Abstract

Plasma spraying of cast iron powder (grit) containing 2.64 % C was investigated. A water-stabilized plasma torch was employed in spraying. Some characteristics of molten particles flying in the plasma stream were measured at various distances from the powder injector, in particular average surface temperature and average velocity. Oxidation and decarburization accompanying the flight of molten cast iron particles in the plasma stream were studied by determining the oxygen and carbon concentrations before and after the in-flight spraying period. At the latter moment, the reactions were stopped by trapping the particles in liquid nitrogen. Significant effects of the powder feed rate and the feeding distance on oxidation and decarburization were observed. X-ray diffraction and Mössbauer spectroscopy yielded some information on the structure changes of cast iron particles during the in-flight period of plasma spraying.

K e y w o r d s: cast iron powder, plasma spraying, oxidation, decarburization

1. Introduction

Air plasma spraying of metals is accompanied by reactions of molten metal powder with the ambient gas. The whole plasma spraying process consists of two stages. At the first of them (in-flight stage), the particles are molten and carried by the plasma stream. The second stage starts at the moment of particle impact and solidification. This stage lasts till the formation and cooling of a plasma deposit (coating) on a substrate. The present paper describes some phenomena occurring during the first (in-flight) stage.

Due to air entrainment into the plasma stream, the most frequently observed reaction is oxidation of metallic particles. Besides, the alloys containing higher amounts of carbon may exhibit decarburization during plasma spraying. In addition, selective vaporization of some alloying elements may occur. In general, various alloying elements are consumed at various rates during plasma spraying, which results in alloy composition changes.

The aim of this paper is to show how simultaneous oxidation and decarburization of cast iron powder are affected by the main plasma spraying parameters. Cast iron was chosen because it can serve as kind of standard alloy containing relatively high amount of carbon, which enables investigating both reactions during spraying. These reactions were studied in the present work preferably, whereas the metallurgical properties of plasma sprayed cast iron were not of special interest.

The two reactions, oxidation and decarburization, presumably occur especially at very high temperatures. That is why the first (in-flight) stage was only studied, where all reactions are of the type gas – liquid (i.e. melt).

Plasma spraying of cast iron has been reported scarcely in the literature. Some properties of plasma sprayed and flame sprayed cast iron have been compared in [1, 2]. Other papers deal mainly with individual splats obtained from cast iron powder particles [3–6].

An attempt was made to determine some parameters of the flying molten particles such as their surface temperature, velocity and size. These characteristics of various materials sprayed by gas-stabilized plasma

*Corresponding author: tel.: +420 266 053 917; fax: +420 286 586 389; e-mail address: volenik@ipp.cas.cz

torches have been reported in a number of papers during the last 15 years. Among them, [7–9] can be mentioned. For spraying by a water-stabilized plasma torch, the relevant data have only been obtained recently for a few selected powder materials [10–12].

2. Experimental

2.1. Material

Cast iron grit delivered by Slezský Kámen Co., Jeseník, was employed as feedstock powder. The particle size obtained by sieving was $-140 + 100$ μm. Among elemental composition data, the concentrations of carbon (2.64 % by mass), oxygen (0.31 %), silicon (1.75 %), and also nitrogen (0.004 %) were of interest. The order of magnitude of impurity levels was 0.1 % and less.

2.2. Plasma spraying

The feedstock powder was plasma sprayed by a 160 kW water-stabilized plasma torch WS® 500. The powder feeding gas was argon. The powder feed rate was either $5\,\mathrm{kg\,h^{-1}}$ or $30\,\mathrm{kg\,h^{-1}}$. Two values of the feeding distance FD (torch nozzle – powder injector) were tested, namely 75 and 125 mm. To stop all high-temperature reactions immediately after the in-flight stage and to obtain the particles for analysis, the axis of the torch was positioned vertically and the flying molten particles were trapped and quenched in liquid nitrogen. The average spraying distance SD (nozzle – liquid nitrogen level) was 430 mm. The liquid nitrogen level fell rapidly during the spraying run lasting ≈ 25 s. The difference between the nitrogen levels at the beginning and at the end of a spraying run depended on the powder feed rate. For $5\,\mathrm{kg\,h^{-1}}$ it was ≈ 60 mm. To maintain the required average spraying distance, the spraying began at SD ≈ 400 mm in this case. For $30\,\mathrm{kg\,h^{-1}}$, the difference was ≈ 80 mm and it was necessary to start at SD ≈ 390 mm.

2.3. Measurements

The main object of the study was cast iron powder after the in-flight stage of plasma spraying. The changes of powder composition occurring during this stage were assessed by comparing with the unsprayed feedstock powder.

To characterize the in-flight stage itself, some parameters of the flying particles were measured. For this purpose, a plasma spray diagnostic system DPV-2000 (Tecnar Automation Ltd.) was employed to determine the particle velocity, surface temperature and size. The device uses thermal radiation emitted from the flying particles to measure their characteristics. The system utilizes an automatic procedure, which scans a plane perpendicular to the particle flow in a stepwise manner to determine the distribution of mean particle parameters in this plane and to find the point of the highest particle flow ("centre point"). The scan plane area of 60×60 mm consisted of 4×4 steps separated by 20 mm. The measured volume size in each of these fields was about $2 \times 2 \times 5\,\mathrm{mm^3}$. Each volume was measured for 5 s. The measurement cannot be conducted near the plasma torch nozzle because of strong plasma radiation. The shortest acceptable flight distance (from the powder injector) was 225 mm, i.e. 300 or 350 mm from the nozzle. After the measurement of the scan plane, these distances were increased by 70 mm and another plane was scanned. This was repeated several times to reach the final distance of > 500 mm from the nozzle.

Oxidation, decarburization and to some extent also nitridation contributed to the changes during the in-flight stage. These were characterized by elemental analysis conducted by "extractive fusion" (LECO method). The concentrations of carbon, nitrogen and oxygen were determined in this way.

A detailed investigation of phases present in the samples after the in-flight stage of plasma spraying was not the main object of this work. Nevertheless, to obtain some qualitative information, X-ray diffraction (filtered Co radiation) as well as ^{57}Fe Mössbauer spectroscopy with detection of 14.4 keV gamma radiation in scattering mode were applied. For the interpretation of diffraction results, the peak positions were compared with the data base PDF 2 – ICDD.

To analyse qualitatively the non-metallic species present in the samples, the metallic phase was dissolved entirely in an iodine-methanol solution. The procedure was described in [13]. To obtain a sufficient amount of extracted non-metallic species, the powders sprayed at $30\,\mathrm{kg\,h^{-1}}$ were only selected for this treatment.

3. Results

The shapes of the feedstock powder particles were highly irregular, which is typical of cast iron grit. During the in-flight stage of plasma spraying, significant spheroidization took place.

The results of particle surface temperature and velocity measurements are shown in Figs. 1, 2. The reason for including the plots obtained at the feed rate $16\,\mathrm{kg\,h^{-1}}$ is explained below. The size measurement served for evaluating the mean diameter of detected particles, i.e. melt drops flying in the plasma stream. The resulting values at $5\,\mathrm{kg\,h^{-1}}$ were as follows: 92.5 μm for FD 75 mm, 100.8 μm for FD 125 mm. The mean diameters enable comparison of individual spraying runs at varying parameters. However, with

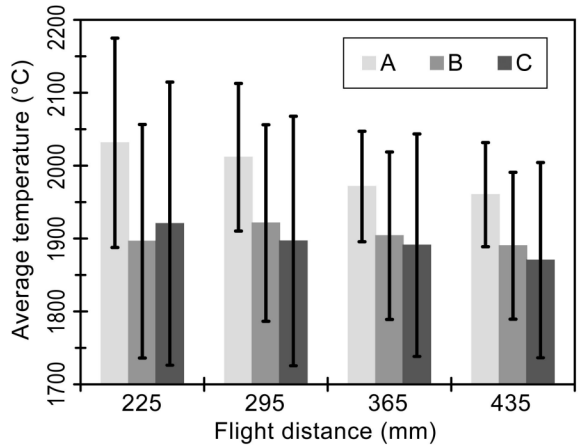

Fig. 1. Plot of average particle surface temperatures as measured by DPV-2000 at different flight distances during plasma spraying at three different conditions: A – feeding distance 75 mm, feed rate 5 kg h^{-1}; B – feeding distance 125 mm, feed rate 5 kg h^{-1}; C – feeding distance 125 mm, feed rate 16 kg h^{-1}. Each column of a triad relates to the same flight distance indicated below the graph. The error bars correspond to standard deviations averaged over the 16 (4 × 4) fields of measurement for the given flight distance.

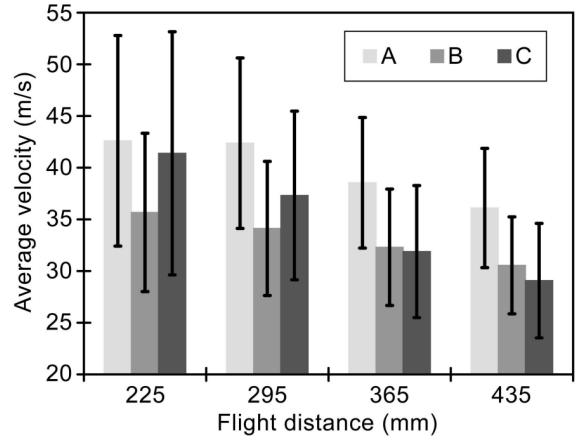

Fig. 2. Plot of average particle velocities as measured by DPV-2000 at different flight distances during plasma spraying at three different conditions: A – feeding distance 75 mm, feed rate 5 kg h^{-1}; B – feeding distance 125 mm, feed rate 5 kg h^{-1}; C – feeding distance 125 mm, feed rate 16 kg h^{-1}. Each column of a triad relates to the same flight distance indicated below the graph. The error bars correspond to standard deviations averaged over the 16 (4 × 4) fields of measurement for the given flight distance.

Table 1. Typical average concentration values (% by mass) of carbon, nitrogen and oxygen in cast iron powder after the in-flight stage of spraying

Feed rate (kg h^{-1})	FD (mm)					
	75			125		
	C	N	O	C	N	O
5	0.28	0.35	3.54	1.00	0.15	1.35
30	0.96	0.05	1.06	2.05	0.03	0.78

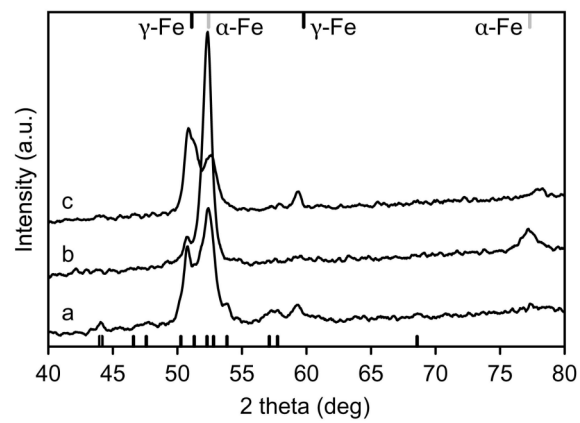

Fig. 3. X-ray diffraction (XRD) patterns of cast iron feedstock powder and selected powder samples sprayed into liquid nitrogen (feed rate 30 kg h^{-1}): a – feedstock powder; b – powder sprayed at feeding distance 75 mm; c – powder sprayed at feeding distance 125 mm. Standard positions of XRD peaks/lines of α- and γ-Fe phases are indicated. Short strokes at the bottom of the graph denote the main standard XRD lines of cementite (Fe_3C).

respect to somewhat arbitrary calibration of the DPV size measurements, no quantitative relationship to the feedstock powder size can be derived from the results.

At high powder feed rate of 30 kg h^{-1}, the DPV cannot distinguish small particles from the high radiation background produced by a large number of particles in the stream. At this feeding rate, the device registers preferably the larger particles. If the feed rate was approximately a half (16 kg h^{-1}) of this maximum value, the DPV measurement was applicable and the mean particle diameter was 97.0 μm. This case is presented in Figs. 1, 2 just to show the extent of particle velocity and temperature changes if the feed rate is increased.

In Table 1, typical results of carbon, nitrogen and oxygen determination in the powder after the in-flight stage of plasma spraying are given. The results obtained by the LECO method are average values of 4 independent measurements including independent sampling.

In Fig. 3, X-ray diffraction patterns of unsprayed cast iron (feedstock powder) and selected plasma sprayed powder samples (powder feed rate 30 kg h^{-1}) are presented. Figure 4 shows X-ray diffraction patterns of extracted non-metallic phases. The Mössbauer

Table 2. Interpretation of Mössbauer spectra shown in Fig. 5. I – relative intensity (with respect to the total spectrum) of the partial spectrum of a phase; B_{hf} – hyperfine induction; IS – isomer shift; QS – quadrupole splitting; I_p – relative intensity of a spectral component with respect to the partial spectrum of the phase. The values of I are identical with relative concentrations (atomic fractions) of phases in the samples on the assumption that the Lamb-Mössbauer factors (f-factors) of all phases are the same

Phase	I feed-stock powder	I FD 75	I FD 125	Component	B_{hf} (T)	IS (mm s^{-1})	QS (mm s^{-1})	I_p feed-stock powder	I_p FD 75	I_p FD 125
α-Fe	0.53±0.01	0.87±0.02	0.62±0.01	1st sextet	33.1±0.05	0.12±0.01	0.12±0.01	0.58±0.01	0.80±0.02	0.72±0.01
				2nd sextet	30.2±0.12	0.12±0.01	0.12±0.01	0.28±0.01	0.14±0.02	0.18±0.02
				3rd sextet	26.1±0.32	0.12±0.01	0.12±0.01	0.14±0.02	0.06±0.02	0.10±0.02
γ-Fe	0.19±0.01	0.08±0.01	0.24±0.01	singlet	–	0.09±0.02	–	0.39±0.02	0.37±0.02	0.34±0.02
				doublet	–	0.11±0.02	0.64±0.06	0.61±0.02	0.63±0.02	0.66±0.02
Fe_3C	0.28±0.01	0.05±0.01	0.14±0.01	sextet	20.4±0.10	0.19±0.01	0.02±0.01			

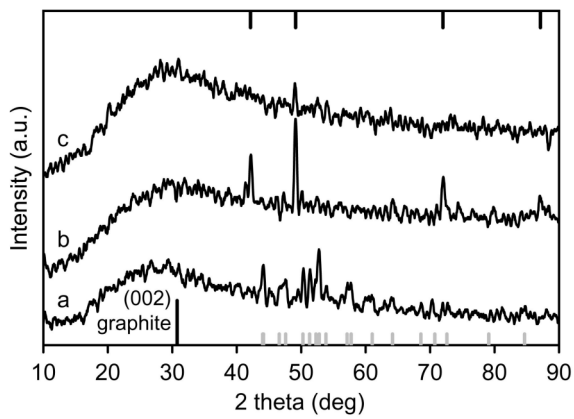

Fig. 4. X-ray diffraction (XRD) patterns of non-metallic phases extracted from feedstock powder and from selected powder samples sprayed into liquid nitrogen (feed rate 30 kg h^{-1}): a – extract from feedstock powder of cast iron; b – extract from powder sprayed at feeding distance 75 mm; c – extract from powder sprayed at feeding distance 125 mm. Standard positions of XRD lines of wüstite ("FeO") are indicated at the top of the graph. At the bottom, besides the position of the only significant standard graphite XRD line, standard lines of cementite (Fe_3C) are denoted.

spectra of the same samples as in Fig. 3 are in Fig. 5. Their interpretation is listed in Table 2. The results yielded by both methods are in good qualitative agreement because both of them show the presence of α-Fe, γ-Fe and Fe_3C. The latter two species were pronounced in the feedstock powder and in the powder sprayed at FD 125 mm, whereas the highly decarburized powder sprayed at FD 75 mm (see Table 1) was composed of almost pure α-Fe. It can be assumed that this also holds for samples sprayed at 5 kg h^{-1}.

In the mixture of non-metallic phases extracted from the samples, cementite and in more oxidized samples also wüstite ("FeO") were identified by X-ray diffraction, whereas no graphite was found. The sampling of non-metallic phases required a sufficient amount of sprayed cast iron powder, which is difficult to obtain at the low feed rate of 5 kg h^{-1}. That is why the X-ray diffraction patterns and Mössbauer spectra of samples sprayed at 30 kg h^{-1} are only presented. No significant structure difference due to the two feed rate values is expected. The character of the X-ray diffraction patterns, in particular a very broad diffraction maximum in the range of low diffraction angles (Fig. 4) and the absence of the only characteristic intense graphite line, suggest that carbon not bound in cementite was amorphous even in the unsprayed feedstock powder. In plasma sprayed cast iron, this was obviously due to very rapid quenching of the molten particles in liquid nitrogen. The technique of the feedstock powder (grit) production is also characterized by rapid cooling (in water).

4. Discussion

Oxidation and decarburization take place simultaneously during the in-flight stage of plasma spraying. Both reactions are significant especially for low powder feed rate (5 kg h^{-1}).

In addition to these reactions, iron vaporization occurs. If it is very rapid, an enrichment of the alloy in carbon might be expected. However, the present spraying conditions always resulted in carbon depletion. Unfortunately, the absolute vaporization rate of iron could not be determined experimentally.

The surface temperature of flying particles is of primary importance. Not only the average surface temperature but also the mean particle velocity and diameter were determined. The high scatter of results seen in Figs. 1 and 2 is due to strong variations of particle trajectories in the plasma stream. As mentioned above, the measurement is not possible in the region of flying distances up to ≈ 220 mm. The point at which the particles melt is not known either.

The powder feed rate and the feeding distance strongly affected oxidation and decarburization. At a high powder feed rate (30 kg h^{-1}), both reactions were relatively slow. For oxidation this can be qualitatively explained by a smaller amount of oxygen available for the reaction with a surface area unit of flying drops. For decarburization, the explanation may be similar.

It appears that oxidation and decarburization depended significantly not only on the powder feed rate but also on the feeding distance if the spraying distance defined above was kept constant. For low FD, the feedstock powder was injected into a plasma region not far from the plasma gun nozzle where the plasma temperature was very high. Both oxidation and decarburization were rapid at these conditions. For higher FD, both reactions were slower because of the lower plasma temperature. Besides, the abovementioned definition of SD means that the particle trajectories were shorter in this case.

A similar dependence of nitrogen concentration increase on the powder feed rate and the feeding distance was observed. This increase is due to the reaction not only with the entrained atmospheric nitrogen but also with liquid nitrogen at the first moment of its contact with hot (molten) particles. In [14], a model is presented enabling calculation of the cooling rate of particles sprayed into liquid nitrogen.

Though a detailed study of phases present in cast iron powder before and after the in-flight stage of spraying was not the object of this work, some qualitative conclusions can be drawn from the measurements. All samples contained α-Fe, γ-Fe and nonmetallic phases.

In the Mössbauer spectrum, the α-Fe and γ-Fe phases are represented by three and two components, respectively. The 1st, 2nd and 3rd sextets in α-Fe represent iron atoms with 0, 1 and 2 atoms of alloying elements and impurities (AEI) in the nearest neighbourhood. The distribution of intensities I_p of the sextets corresponds to the AEI concentrations. Carbon and silicon are the dominant AEI atoms in the present samples. A rough analysis shows that the higher the concentration of AEI in a solid solution of α-Fe, the lower the I_p ratio of the 1st and 2nd sextets. From this point of view the present results are in agreement with the changes of the carbon concentration in the samples.

The γ-Fe phase is represented by one singlet and one doublet, though due to their overlapping they are not seen clearly in the γ-Fe spectrum. The singlet corresponds to the iron atoms with 0 or one carbon atom, the doublet to iron atoms with 2 carbon atoms in the nearest neighbourhood [15]. The feedstock powder has the lowest carbon concentration in the γ-phase because its important part appears in cementite Fe_3C.

Among the non-metallic phases, crystallographically defined graphite was found neither in the feedstock grit nor in the sprayed powder. Instead, a species that can be denoted as "amorphous carbon" was present in all samples, which is due to rapid cooling both in the production of feedstock powder and in liquid nitrogen quenching of plasma sprayed particles. Even if the total carbon content fell, amorphous carbon was still present (Fig. 4), whereas the Fe_3C amount decreased. Decarburization was very strong and in most cases the sprayed material could not be taken for cast iron any more. Though the surface temperature of the flying particles at distances up to $\approx$ 220 mm from the injector was not known, it could hardly reach a value at which significant vaporization of carbon occurs. Instead, carbon (or more likely cementite) would react with oxygen to produce gaseous carbon oxides. Decomposition of cementite may contribute to this reaction. If a smaller "specific" amount of oxygen is available (in case of 30 kg h^{-1}), the reaction is slower than at 5 kg h^{-1}. To verify the possible decarburizing mechanism based on a reaction of cementite with oxygen, a separate study would be required.

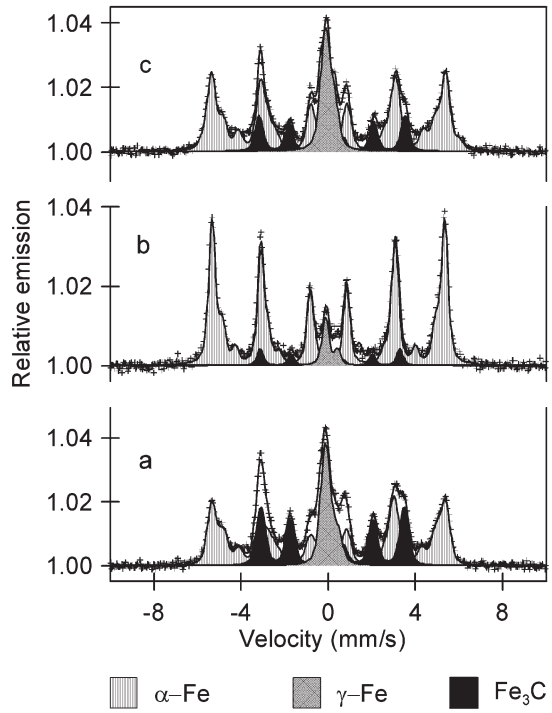

Fig. 5. Mössbauer spectra of feedstock powder and selected powder samples sprayed into liquid nitrogen (feed rate 30 kg h^{-1}): a – feedstock powder; b – powder sprayed at feeding distance 75 mm; c – powder sprayed at feeding distance 125 mm. The spectra are fitted so as to show spectral components corresponding to α-Fe, γ-Fe and Fe_3C. For their parameters, see Table 2.

5. Conclusions

1. Cast iron grit was sprayed using a water-

stabilized plasma torch. To obtain samples for estimating in-flight oxidation and decarburization, the molten particles flying in the plasma stream were trapped and quenched in liquid nitrogen.

2. The parameters of the flying particles were characterized by a device enabling analysis of particle size, surface temperature and velocity. The measurements were limited to low particle flow rate and to a region somewhat distant from the plasma gun nozzle and powder injectors.

3. For a high powder feed rate, both oxidation and decarburization reactions were slow. As a result, the in-flight composition changes of the powder were less significant than for low feed rate. The reason is obviously the amount of entrained oxygen per unit surface area of the flying melt drops.

4. Both reactions were slow at a large feeding distance. This was due to the fact that the powder was fed into relatively cold plasma. The reaction rates were enhanced if decreasing the feeding distance at a constant spraying distance.

5. Both the metallic and non-metallic phases present after the in-flight period in the powder were identified qualitatively.

Acknowledgements

This work was supported by the Academy of Sciences of the Czech Republic, Institutional Research Project No. AV0Z20430508 and grant IAA1041404.

The participation of J. Svatoň, ŽĎAS Company, Žďár nad Sázavou, who performed the LECO measurements, is gratefully acknowledged.

References

[1] MURAKAMI, K.—NAKAZONO, S.—OKAMOTO, T.: Mater. Sci. Eng., *A 108*, 1989, p. 271.

[2] MURAKAMI, K.—OKAMOTO, T.—MIYAMOTO, Y.—NAKAZONO, S.: Mater. Sci. Eng., *A 117*, 1989, p. 207.

[3] MORKS, M. F.—TSUNEKAWA, Y.—OKUMIYA, M.—SHOEIB, M. A.: In: Proc. Thermal Spray 2001: New Surfaces for a New Millenium. Eds.: Berndt, C. C., Khor, K. A., Lugscheider, E. F. Materials Park, OH, ASM International 2001, p. 829.

[4] MORKS, M. F.—TSUNEKAWA, Y.—OKUMIYA, M.—SHOEIB, M. A.: J. Thermal Spray Technol., *11*, 2002, p. 226.

[5] MORKS, M. F.—TSUNEKAWA, Y.—OKUMIYA, M.—SHOEIB, M. A.: J. Thermal Spray Technol., *12*, 2003, p. 282.

[6] MORKS, M. F.—TSUNEKAWA, Y.—OKUMIYA, M.—SHOEIB, M. A.: Mater. Transactions, *44*, 2003, p. 743.

[7] FINCKE, J. R.—SWANK, W. D.—HAGGARD, D. C.: Plasma Chem. & Plasma Processing, *13,* 1993, p. 579.

[8] VARDELLE, M.—VARDELLE, A.—FAUCHAIS, P.: J. Thermal Spray Technol., *2*, 1993, p. 79.

[9] SCHUTZ, M.—BARBEZAT, G.—FLUCK, E.: In: Proc. Thermal Spray, Meeting the Challenges of the 21st Century 1998. Ed.: Coddet, C. Materials Park, OH, ASM International 1998, p. 761.

[10] MATĚJÍČEK, J.—CHUMAK, O.—KONRÁD, M.: In: Proc. Internat. Thermal Spray Conf. 2005. Ed.: Lugscheider, E. Düsseldorf, Verlag für Schweißen und verwandte Verfahren, DVS-Verlag GmbH 2005, p. 594 (CD-ROM).

[11] MATĚJÍČEK, J.—NEUFUSS, K.—KOLMAN, B.—CHUMAK, O.—BROŽEK, V.: In: Proc. Internat. Thermal Spray Conf. 2005. Ed.: Lugscheider, E. Düsseldorf, Verlag für Schweißen und verwandte Verfahren, DVS-Verlag GmbH 2005, p. 634 (CD-ROM).

[12] CHRÁSKA, T.—NEUFUSS, K.—OBERSTE-BERGHAUS, J.—LAMONTAGNE, M.—MOREAU, C.: In: Proc. Internat. Thermal Spray Conf. 2005. Ed.: Lugscheider, E. Düsseldorf, Verlag für Schweißen und verwandte Verfahren, DVS-Verlag GmbH 2005, p. 1292 (CD-ROM).

[13] VOLENÍK, K.—LEITNER, J.—HANOUSEK, F.—DUBSKÝ, J.—KOLMAN, B.: J. Thermal Spray Technol., *6*, 1997, p. 327.

[14] KOTALÍK, P.—VOLENÍK, K.: J. Phys. D: Appl. Phys., *34*, 2001, p. 567.

[15] RON, M.: In: Applications of Mössbauer Spectroscopy. Vol. 2. Ed.: Gonser, U. New York, Academic Press 1980, p. 3.